

SECTION LISTING

BROWSE VOLUMES

Year Range: 2003-2012

Volume 100 2012

Issue 1 | 2 Jan | 01xxxx

Volume 99 2011

Volume 98 2011

Volume 97 2010

Volume 96 2010

Volume 95 2009

Volume 94 2009

Volume 93 2008

Volume 92 2008

Volume 91 2007

Volume 90 2007

Volume 89 2008

Volume 88 2008

Volume 87 2005

Volume 86 2005

Volume 85 2004

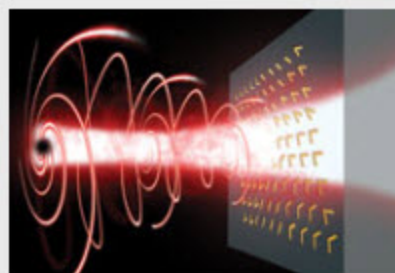
Volume 84 2004

Volume 83 2003

Volume 82 2003

2 Jan 2012

Volume 100, Issue 1, Articles (01xxxx)


 Appl. Phys. Lett. **100**, 013101 (2012);
 doi:10.1063/1.3673334 (3 pages)

 Patrice Genevet, Nanfang Yu, Francesco Aieta, Jiao Lin,
 Mikhail A. Kats, Romain Blanchard, Marlan O. Scully, Zeno
 Gaburro, and Federico Capasso

[Enlarge Image](#) | [Read More](#)

Page 3 of 4 Pages

[Previous Page](#) [Next Page](#) | [Jump to Page](#) 3

 SELECTED: [Export Citations](#) | [Show/Hide Summaries](#) | [Add to MyArticles](#) | [Email](#)

Add View

 NANOSCALE SCIENCE AND TECHNOLOGY

TOP

 Efficiency enhancement of InGaN multi-quantum-well solar cells via light-harvesting SiO₂ nano-honeycombs

P. H. Fu, G. J. Lin, C. H. Ho, C. A. Lin, C. F. Kang, Y. L. Lai, K. Y. Lai, and J. H. He

 Appl. Phys. Lett. **100**, 013105 (2012); doi:10.1063/1.3673838 (4 pages)

Online Publication Date: 4 January 2012

 Full Text: [Read Online \(HTML\)](#) | [Download PDF](#)

 + [Show Abstract](#)

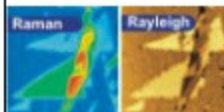
 + [Show PACS](#)
 Thermal effects on the characteristic Raman spectrum of molybdenum disulfide (MoS₂) of varying thicknesses

S. Najmaei, Z. Liu, P. M. Ajayan, and J. Lou

 Appl. Phys. Lett. **100**, 013106 (2012); doi:10.1063/1.3673907 (4 pages)


ADVERTISEMENT

GRAPHENE



One sample in all techniques:

- AFM
- SNOM
- Raman
- TERS



NT-MDT

**AIP
Conference
Proceedings**

 Enjoy fast,
 cost-effective
 publication of
 your meeting's
 key research!

AIP | Publishing

Role of n-dopant based electron injection layer in n-doped organic light-emitting diodes and its simple alternative

Young Wook Park, Jin Hwan Choi, Tae Hyun Park, Eun Ho Song, Hakkoo Kim et al.

Citation: *Appl. Phys. Lett.* **100**, 013312 (2012); doi: 10.1063/1.3674960

View online: <http://dx.doi.org/10.1063/1.3674960>

View Table of Contents: <http://apl.aip.org/resource/1/APPLAB/v100/i1>

Published by the [American Institute of Physics](#).

Related Articles

Barrierless hole injection through sub-bandgap occupied states in organic light emitting diodes using substoichiometric MoO_x anode interfacial layer
[Appl. Phys. Lett.](#) **100**, 013311 (2012)

Surface plasmon-enhanced electroluminescence in organic light-emitting diodes incorporating Au nanoparticles
[Appl. Phys. Lett.](#) **100**, 013308 (2012)

Surface plasmon-enhanced electroluminescence in organic light-emitting diodes incorporating Au nanoparticles
[APL: Org. Electron. Photonics](#) **5**, 8 (2012)

Role of n-dopant based electron injection layer in n-doped organic light-emitting diodes and its simple alternative
[APL: Org. Electron. Photonics](#) **5**, 12 (2012)

Barrierless hole injection through sub-bandgap occupied states in organic light emitting diodes using substoichiometric MoO_x anode interfacial layer
[APL: Org. Electron. Photonics](#) **5**, 11 (2012)

Additional information on *Appl. Phys. Lett.*

Journal Homepage: <http://apl.aip.org/>

Journal Information: http://apl.aip.org/about/about_the_journal

Top downloads: http://apl.aip.org/features/most_downloaded

Information for Authors: <http://apl.aip.org/authors>

ADVERTISEMENT

**AIP Advances**

Submit Now

**Explore AIP's new
open-access journal**

- **Article-level metrics
now available**
- **Join the conversation!
Rate & comment on articles**

Role of n-dopant based electron injection layer in n-doped organic light-emitting diodes and its simple alternative

Young Wook Park,¹ Jin Hwan Choi,¹ Tae Hyun Park,¹ Eun Ho Song,¹ Hakkoo Kim,¹ Hyun Jun Lee,¹ Se Joong Shin,¹ Byeong-Kwon Ju,^{1,a)} and Won Jun Song²

¹Display and Nanosystem Laboratory, College of Engineering, Korea University, Seoul 136-713, South Korea

²Samsung Mobile Display, Yongin-City, Gyeonggi-do 446-711, South Korea

(Received 21 August 2011; accepted 12 December 2011; published online 6 January 2012)

We investigate the enhancement mechanism of the electroluminescence (EL) of alkali metal based n-doped organic light-emitting diodes (OLEDs). The dual role of the n-dopant (carrier transport and lowering of the injection barrier) induces a trade-off. When the electron transport layer (ETL) is optimally doped by the n-dopant for the highest conductivity, the amount of n-dopant at the ETL/cathode interface is insufficient to form enough chemical bonds with the cathode for efficient carrier injection. This insufficient amount of n-dopant limits the carrier injection properties. To solve this problem, we demonstrated that the addition of an electron injection layer (EIL) comprised of the n-dopant could increase its presence at the interface and, thereby, improve the carrier injection properties and, consequently, the EL efficiency. Moreover, simply using an alkali-metal alloy (rather than co-deposition) on the n-doped ETL as a cathode, instead of using the additional EIL, greatly improves the EL efficiency of the OLEDs. The alkali-metal alloy cathode increased the interfaced states at the ETL/cathode. The proposed model was confirmed by x-ray photoemission spectroscopy experiments on the alkali-metal n-dopant/electrode interface. © 2012 American Institute of Physics. [doi:10.1063/1.3674960]

Electrical doping methods have been widely investigated in order to improve the electroluminescent (EL) efficiency of organic light-emitting diodes (OLEDs). Metal oxide and alkali metal based doping methods are considered to be a promising way to derive enhanced charge injection from the contacts and to reduce the ohmic losses. Metal oxides, such as WO₃ (Ref. 1), V₂O₃ (Ref. 2), MoO₃ (Ref. 3), and ReO₂ (Ref. 4), have been used as the p-type dopant in the hole transport layers. Conversely, Cs (Ref. 5), Cs₂CO₃ (Ref. 6), CsN₃ (Ref. 7), and Rb₂CO₃ (Ref. 8) have been used as the n-type dopant in the electron transport layers (ETLs).

The mechanism of enhancement underlying n-doping based on alkali metals is still open to dispute due to their high reactivity.^{6,9,10} However, they are known to enhance the carrier transport at the n-doped ETL and improve the carrier injection at the ETL/cathode interface.^{5,6,11} In the case of n-doped ETL, the excess carriers in the matrix donated by the doped Cs enhance the conductivity,⁴ while, in the case of Cs₂CO₃ doping, there is a possibility that Cs metal or Cs based oxide derivatives are formed and, subsequently, react with the Al cathode to produce Cs-Al or Cs-O-Al, as reported in Refs. 5 and 6.

In this work, we focused on the correlation between the two roles of the n-dopant in the ETL, viz., the enhancement of the carrier transport of the ETL and of the carrier injection at the ETL/cathode interface. Since its optimal doping concentration is mainly determined by the carrier transport properties of the doped ETL, but the concentration of n-dopant at the optimally doped ETL/cathode interface is likely to be insufficient to form enough chemical bonds with the cathode

for efficient carrier injection. This insufficient presence could be solved by applying an additional n-dopant based electron injection layer (EIL). We demonstrated that an OLED having the structure of the optimally n-doped ETL/n-dopant based EIL/cathode showed improved EL characteristics. Moreover, we demonstrated that the simple use of an alkali-metal alloy instead of the additional n-dopant based EIL could improve the EL characteristics of the n-doped OLED. Since alkali-metals (R) are reported to form R-O-Al or R-Al,^{5,6} thereby increasing the carrier injection, the n-doped OLEDs utilizing an alkali-metal aluminum alloy showed improved EL characteristics compared to the conventional aluminum cathode structure, while the alkali-metal alloy already has R-Al (Li-Al bond, during the synthesis of the alloy metal). In this investigation, we compared the OLEDs devices using either intrinsic or n-doped Bphen ETL, an additional n-dopant (Cs₂CO₃) based EIL, and by changing the material type of the cathode (Al or LiAl). The studies were performed by x-ray photoemission spectroscopy experiments on the alkali-metal based n-dopant/electrode interface.

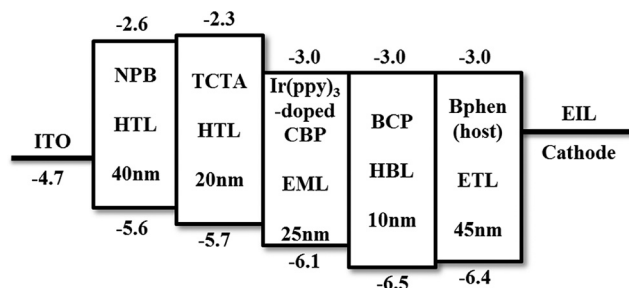


FIG. 1. The energy level diagram and device structure of the fabricated OLEDs.

^{a)} Author to whom correspondence should be addressed. Electronic mail: bkju@korea.ac.kr. Tel.: +82-2-3290-3237. FAX: +82-2-3290-3791.

TABLE I. Device configurations.

Configuration	Structure: from ETL to cathode
Device—Reference	Bphen/LiF/Al
Device—R_EIL/Al	Bphen/Cs ₂ CO ₃ /Al
Device—R_EIL/LiAl	Bphen/Cs ₂ CO ₃ /LiAl
Device—N_Al	Bphen:Cs ₂ CO ₃ /Al
Device—N_EIL/Al	Bphen:Cs ₂ CO ₃ /Cs ₂ CO ₃ /Al
Device—N_LiAl	Bphen:Cs ₂ CO ₃ /LiAl

The structure and energy band diagram of the fabricated optimized OLEDs are shown in Figure 1 and Table I. The devices have different ETLs to cathode structures. They utilize the same structure from the anode to the hole blocking layer (HBL); 40 nm of 4,4'-bis[*N*-(1-naphthyl)-*N*-phenylamino] biphenyl (NPB) for the hole injection and transport layers, 20 nm of 4,4',4''-tris(*N*-carbazolyl)-triphenyl-amine (TCTA) for the hole transport and exciton blocking layers, 25 nm of 7 wt. % tris(2-phenylpyridine)iridium(III) [Ir(ppy)₃] doped *N,N'*-dicarbazolyl-4-4'-biphenyl (CBP) for the emission layer (EML), and 10 nm of 2,9-dimethyl-4,7-diphenyl-1,10-phenanthroline (BCP) for the HBL. For the ETL, 4,7-diphenyl-1,10-phenanthroline (Bphen) and Cs₂CO₃ were used as the host and n-dopant, respectively. The thickness of the ETL was 45 nm and the n-doping concentration was 15 wt. %, which was optimized for the highest conductivity and EL characteristics. 0.8 nm of lithium fluoride (LiF) and 1.6 nm of Cs₂CO₃ were used as the EIL, which was also optimized for the highest carrier injection and EL characteristics. The thickness and doping concentrations were obtained from the literature and optimized. Lithium-aluminum alloy (LiAl) was commercially purchased and used as the alkali-metal aluminum alloy. We present here the 6 optimized devices: “Device—Reference” having an intrinsic Bphen ETL/LiF EIL/Al cathode, “Device—R_EIL/Al” having an intrinsic Bphen ETL/Cs₂CO₃ EIL/Al cathode, “Device-R_EIL/LiAl” having an intrinsic Bphen ETL/Cs₂CO₃ EIL/LiAl cathode, “Device—N_Al” having an n-doped ETL/Al cathode, “Device—N_EIL/Al” having an n-doped ETL/Cs₂CO₃ EIL/Al cathode, and “Device—N_LiAl” having an n-doped ETL/LiAl cathode.

The OLEDs were fabricated on ITO coated glass purchased from Samsung Corning Precision Glass. Before using the ITO coated glass, it was finely cleaned with organic solvents and deionized water. Photo resist was used as an insulating layer to prevent unintentional electrical shorts between the anode and cathode electrodes. Also, an insulating layer was used to define the active area, which for this device is 4 × 4 mm². The organic, inorganic, and cathode layers are subsequently deposited by a thermal evaporator at a base pressure of about 10⁻⁶ Torr where the deposition rates of all of the organic materials and the metal are ~1 Å/s and ~6 Å/s, respectively.

The EL characteristics were measured using a PR-670 SpectraScan Spectroradiometer (Photo Research, Inc.) and a Model 237 High-Voltage Source-Measure Unit (Keithley Instruments, Inc.) in a dark box in an air atmosphere.

To measure the bonding state at the n-doped ETL/cathode interface, x-ray photoelectron spectrometer (XPS) analy-

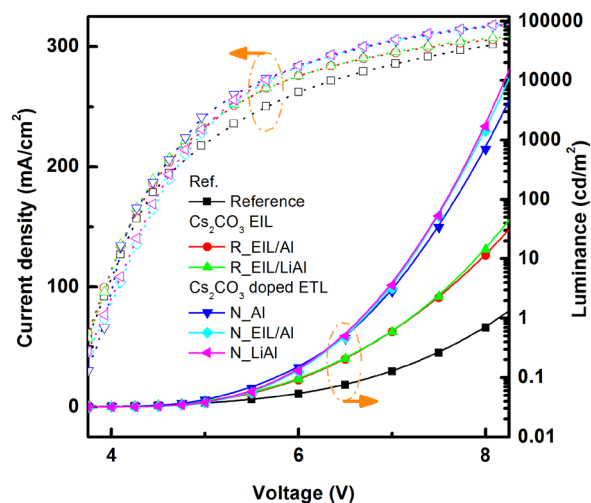


FIG. 2. (Color online) The current density and luminance curve as a function of the applied voltage.

sis was performed with an ESCALAB 250 multifunction x-ray photoelectron spectrometer (Thermo Scientific Inc.) using an Al K α (1486.6 eV) excitation source with the binding energy calibrated to the value of the contaminated carbon (C1s: 284.6 eV).

The EL characteristics of the fabricated OLEDs are shown in Figures 2–4. A summary of the device performance of the OLEDs is found in Table II.

In Figure 2, compared to Device-Ref, all of the other devices show an improved current density at the same bias voltage; the current density-voltage characteristics are in the order of Device-N_LiAl > Device-N_EIL/Al > Device-N_Al \gg Device-R_EIL/LiAl > Device-R_EIL/Al \gg Device-Reference. Also, as represented in Figure 3, the EL efficiency of the devices is enhanced as a result of the improvement in the current density-voltage characteristics.

The OLEDs with the n-doped ETL (Devices N) show a highly improved current density, followed by those with an un-doped ETL/Cs₂CO₃ EIL (Devices R). The difference between Device R and Device-Reference is mainly due to the lowering of the electron injection barrier by the EIL and also to the improved electron transport characteristics

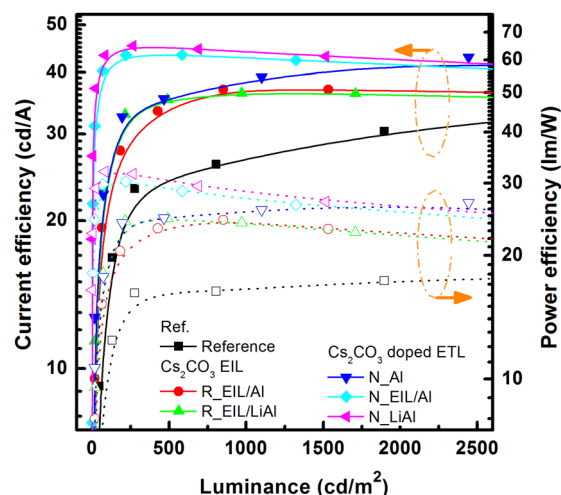


FIG. 3. (Color online) The current efficiency and power efficiency curve as a function of the luminance.

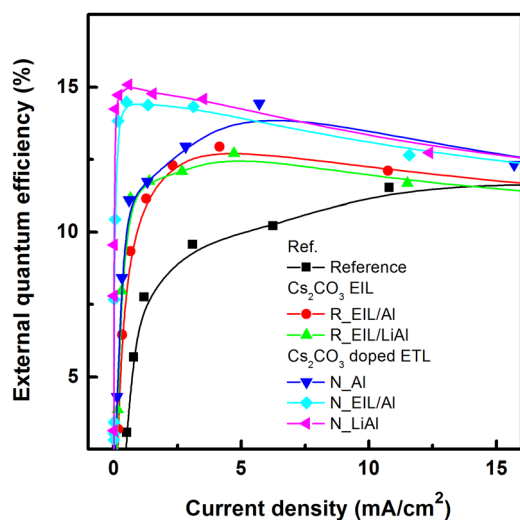


FIG. 4. (Color online) The external quantum efficiency as a function of the driving current density.

afforded by the diffusion of the Cs_2CO_3 into the ETL; however, the difference between Device N and Device-Reference is much larger and this can be attributed to the highly improved electron transport characteristics caused by the Cs_2CO_3 n-doping in the ETL and the improved electron injection characteristics caused by the reaction between the Cs_2CO_3 n-dopant and the cathode at the ETL/cathode interface. The further analysis is as follows.

Based on the previously reported result that the use of less than ~ 5 Cs atomic layers improves the electron injection,⁵ the reaction of the Cs derivatives formed by Cs_2CO_3 deposition with the cathode can result in efficient carrier injection.⁶ Although the Cs_2CO_3 EIL in Devices R_EIL/Al and R_EIL/LiAl efficiently improved the carrier injection, Devices R_EIL/Al and R_EIL/LiAl showed dependence on the cathode material. Device-R_EIL/LiAl having a LiAl cathode shows higher carrier injection characteristics and EL efficiencies in the low current density region of around 1 mA/cm^2 . However, the LiAl cathode has been known to have lower device performance than the LiF/Al cathode in conventional devices (not in P-I-N devices).¹² The former only improved injection mechanism, while the latter has improved injection and transport characteristics afforded by diffusion into the transport layer.^{12–14} These device performances conflict with our results. It is possible to assume that the Cs_2CO_3 EIL reaction at the Al cathode is insufficient, due to the diffusion of Cs_2CO_3 into the ETL. Thus, the LiAl

cathode improves the device efficiency by increasing the reaction possibility of R-Al or R-O-Al or substituting the R-Al or R-O-Al by itself. This assumption becomes clear in Devices N.

The Cs derivatives of the Cs_2CO_3 n-doped ETL in Device-N_Al are supposed to react with the cathode; however, their quantity is insufficient. Thus, the devices having an additional electron injection improvement layer (the Cs_2CO_3 EIL of Device-N_EIL/Al or the LiAl cathode of Device-N_LiAl) show improved overall EL efficiencies compared to the one without them (Device-N_Al). This tendency is the same as that for Devices R. Device-N_LiAl, possessing a LiAl cathode on top of the Cs_2CO_3 n-doped ETL, shows the highest external quantum efficiency (EQE) and power efficiency (PE) of 15% and 30.7 lm/W at 1 mA/cm^2 , an increase of 27% and 30%, respectively, compared to Device-N_Al with the Al cathode. On the other hand, the devices using additional n-dopant based EIL showed the same tendency as the reference devices; the EL efficiency was reduced when the thickness of the EIL was less than or greater than 1.6 nm. Also, the n-dopant based EIL/LiAl cathode device showed higher efficiency than Device-N_Al, but lower efficiency than Device-N_LiAl.

The improved characteristics of the n-doped ETL/LiAl cathode device compared to the other devices were attributed to the enhanced electron injection properties caused by the reaction between the n-doped ETL and the LiAl cathode or doing the same role of R-Al or R-O-Al by already made bonds during the synthesis of LiAl alloy. This enhancement in the EL efficiency by the alkali-metal Al alloy cathode in the n-doped ETL device was also observed in the different alkali metal based n-dopant (NaN_3) doped devices and resulted in both higher carrier injection and EL efficiencies.¹⁵ This result is surprising, since the use of LiAl cathodes in OLEDs having un-doped intrinsic ETL has been reported to give rise to low efficiency compared to the use of LiF/Al cathodes. Thus, the order of carrier injection efficiency for the EIL/cathode of the OLEDs having the n-doped ETL was demonstrated to be $\text{Al} < \text{Cs}_2\text{CO}_3/\text{Al} < \text{LiAl}$, while that of the OLEDs having the un-doped intrinsic ETL was reported to be $\text{Al} < \text{LiAl} < \text{LiF}/\text{Al} < \text{Cs}_2\text{CO}_3/\text{Al}$ in the literature. This difference originates from the trade-off induced by the dual role of the n-dopants, thus an n-dopant based EIL or one using an alkali-metal alloy needs to be used.

In order to analyze the difference in the interfacial states between the n-doped ETL/Al and the n-doped ETL/LiAl structures, XPS was carried out. Since Cs derivatives are

TABLE II. Summary of the performance of the fabricated OLEDs.

Configuration	at Peak EQE (%)		at 1 mA/cm^2		at 500 cd/m^2	
	EQE (%)	J (mA/cm^2)	EQE (%)	PE (lm/W)	EQE (%)	PE (lm/W)
Device—Reference	11.7	18.3	6.8	14.4	8.6	16.2
Device—R_EIL/Al	12.9	4.1	11.1	23.3	11.3	23.5
Device—R_EIL/LiAl	12.7	4.7	11.7	24.6	11.7	24.6
Device—N_Al	14.4	6.0	11.7	24.7	11.7	23.4
Device—N_EIL/Al	14.5	0.5	14.4	29.4	14.4	29.0
Device—N_LiAl	15.1	0.6	15.0	30.7	14.9	30.5

highly unstable in air, due to such effects as deliquescence, not only Cs_2CO_3 , but also the as-deposited Cs derivatives react with the molecules in the atmosphere. In their study, Band *et al.* used a special sample holder to maintain an inert gas atmosphere and sputtered depth-profiling to remove the surface carbon contamination.⁹ We also used the sputtered depth-profiling method. The Cs_2CO_3 (30 nm) and the cathode (Al and LiAl, 100 nm) were sequentially deposited on a Si wafer for the measurement. The metal cathode was also used to prevent the reaction of Cs with the molecules in the atmosphere. The LiAl cathode sample showed different bonding state, as well as improved carrier injection and EL characteristics.¹⁵

In conclusion, we demonstrated the highly improved EL efficiency of n-doped OLEDs utilizing an additional n-dopant based EIL. The addition of the n-dopant based EIL enhanced the R-O-Al or R-Al reactions by increasing the n-dopant concentration at the ETL/cathode interface of the n-doped OLEDs. Moreover, we demonstrated a simple alternative method, viz., using a LiAl alkali-metal aluminum alloy cathode without using an additional n-dopant based EIL. Even though alkali-metal alloy cathodes including LiAl have been reported to have lower efficiency than LiF/Al cathodes in OLEDs having an un-doped intrinsic ETL, the simple use of the alkali-metal alloy cathode instead of the additional n-dopant based EIL improved the injection property at the ETL/cathode interface and resulted in a higher EL efficiency. In addition, the alkali-metal aluminum alloy cathode is superior to the conventional aluminum one in terms of its handling and fabrication, since its reactivity is much lower than that of aluminum and it is resistant to oxidation.

This work was supported by a Korea Science and Engineering Foundation (KOSEF) grant funded by the Korea

Ministry of Education, Science and Technology (MEST) (CAFDC-20100009869) and by the World Class University (WCU, R32-2008-000-10082-0) Project of MEST, as well as by the Industrial Strategic Technology Development Program of MKE (KI002104, Development of Fundamental Technologies for Flexible Combined-Function Organic Electronic Device). We also wish to thank the Korea Basic Science Institute for the use of their XPS equipment.

¹C.-C. Chang, M.-T. Hsieh, J.-F. Chen, S.-W. Hwang, and C.-H. Chen, *Appl. Phys. Lett.* **89**, 253504 (2006).

²T. Matsumoto, T. Nakada, J. Endo, K. Mori, N. Kawamura, A. Yokoi, and J. Kido, *SID Int. Symp. Digest Tech. Papers* **2003**, 979.

³H. Ikeda, J. Sakata, M. Hayakawa, T. Aoyama, T. Kawakami, and K. Kamata, *SID Int. Symp. Digest Tech. Papers* **2006**, 923.

⁴D.-S. Leem, H.-D. Park, J.-W. Kang, J.-H. Lee, J. W. Kim, and J.-J. Kim, *Appl. Phys. Lett.* **91**, 011113 (2007).

⁵T. Oyamada, C. Maeda, H. Sasabe, and C. Adachi, *J. Appl. Phys.* **42**, L1535 (2003).

⁶J. Huang, Z. Xu, and Y. Yang, *Adv. Funct. Mater.* **17**, 1966 (2007).

⁷K. S. Yook, S. O. Jeon, S.-Y. Min, J. Y. Lee, H.-J. Yang, T. Noh, S.-K. Kang, and T.-W. Lee, *Adv. Funct. Mater.* **20**, 1797 (2010).

⁸D.-S. Leem, J.-H. Lee, J.-J. Kim, and J.-W. Kang, *Appl. Phys. Lett.* **93**, 103304 (2008).

⁹A. Band, A. Albu-Yaron, T. Livneh, H. Cohen, Y. Feldman, L. Shimon, R. Popovitz-Biro, V. Lyahovitskaya, and R. Tenne, *J. Phys. Chem. B* **108**, 12360 (2004).

¹⁰M.-H. Chen and C.-I. Wu, *J. Appl. Phys.* **104**, 113713 (2008).

¹¹S.-Y. Chen, T.-Y. Chu, J.-F. Chen, C.-Y. Su, and C. H. Chen, *Appl. Phys. Lett.* **91**, 011113 (2007).

¹²D. H. Chung, S. W. Hur, S. K. Kim, J. U. Lee, C. H. Kim, J. W. Hong, and T. W. Kim, *Curr. Appl. Phys.* **4**, 667 (2004).

¹³I. W. Wu, Y.-H. Chen, P.-S. Wang, C.-G. Wang, S.-H. Hsu, and C.-I. Wu, *Appl. Phys. Lett.* **96**, 013301 (2010).

¹⁴H. Heil, J. Steiger, S. Karg, M. Gastel, H. Ortner, H. von Seggern, and M. Stöbel, *J. Appl. Phys.* **89**, 420 (2001).

¹⁵See supplementary material at <http://dx.doi.org/10.1063/1.3674960> for the EL characteristics of OLEDs with NaN_3 doped ETL of Figure s-1 and s-2 and the XPS results of Cs_2CO_3 /cathode interface of Figure s-3 and s-4.